Glycobiology vol. 22 no. 9 pp. 1183–1192, 2012
doi:10.1093/glycob/cws087
Advance Access publication on May 28, 2012

The C-terminal fragment of axon guidance molecule Slit3 binds heparin and neutralizes heparin's anticoagulant activity

Eduard Condac[2], Heather Strachan[2], Gerardo Gutierrez-Sanchez[2], Benjamin Brainard[3], Christina Giese[4], Christian Heiss[2], Darryl Johnson[2], Parastoo Azadi[2], Carl Bergmann[2], Ron Orlando[2], Charles T Esmon[5], Job Harenberg[4], Kelley Moremen[2], and Lianchun Wang[1,2]

[2]Department of Biochemistry and Molecular Biology, Complex Carbohydrate Research Center, University of Georgia, 315 Riverbend Road, Athens, GA 30602-4712, USA; [3]College of Veterinary Medicine, University of Georgia, Athens, GA, USA; [4]Clinical Pharmacology, Faculty of Medicine Mannheim, Ruprecht-Karls University Heidelberg, Mannheim, Germany; and [5]Coagulation Biology Laboratory, Oklahoma Medical Research Foundation, Oklahoma City, OK, USA

Received on January 1, 2012; revised on April 28, 2012; accepted on May 14, 2012

Slit3 is a large molecule with multiple domains and belongs to axon guidance families. To date, the biological functions of Slit3 are still largely unknown. Our recent study demonstrated that the N-terminal fragment of Slit3 is a novel angiogenic factor. In this study, we examined the biological function of the C-terminal fragment of human Slit3 (HSCF). The HSCF showed a high-affinity binding to heparin. The binding appeared to be heparin/heparan sulfate-specific and depends on the size, the degree of sulfation, the presence of N- and 6-*O*-sulfates and carboxyl moiety of the polysaccharide. Functional studies observed that HSCF inhibited antithrombin binding to heparin and neutralized the antifactor IIa and Xa activities of heparin and the antifactor IIa activity of low-molecular-weight heparin (LMWH). Thromboelastography analysis observed that HSCF reversed heparin's anticoagulation in global plasma coagulation. Taken together, these observations demonstrate that HSCF is a novel heparin-binding protein that potently neutralizes heparin's anticoagulation activity. This study reveals a potential for HSCF to be developed as a new antidote to treat overdosing of both heparin and LMWH in clinical applications.

Keywords: anticoagulation / antithrombin / heparin / neutralization / Slit3

Introduction

The Slit families of axon guidance molecules are large, secreted proteins and are highly conserved from *Caenorhabditis elegans* to vertebrates (Rothberg et al. 1990; Itoh et al. 1998). Mammals have three Slit proteins (Slit1–3). They have an overall 60–66% sequence identity and share a common domain organization: a putative signal peptide at the N terminus followed by a long stretch of four leucine-rich repeats, six epidermal growth factor (EGF)-like domains, an agrin–laminin–perlecan–slit conserved motif, another three EGF-like domains and a cysteine-knot domain at the C terminus (Itoh et al. 1998). A similar domain structure is found in *Drosophila* Slit (dSlit) that has a 43.5, 44.3 and 41.1% sequence homology with mammalian Slit1, Slit2 and Slit3, respectively (Rothberg and Artavanis-Tsakonas 1992; Itoh et al. 1998; Brose et al. 1999). dSlit and bovine Slit2 were shown to be cleaved in vivo by unknown proteases (Brose et al. 1999). In vitro cleavage was also reported for human Slit2 (hSlit2) and hSlit3 expressed in Chinese hasmster ovary (CHO) cells and for hSlit2 and dSlit expressed in COS and human embryonic kidney (HEK) 293 cells (Brose et al. 1999; Patel et al. 2001). Studies of mammalian Slit2 established that Slit2 binds through the second leucine-rich repeat to the appropriate receptors Robo to exert functions as a guidance molecule involved in neuron growth, cell migration and angiogenesis (Howitt et al. 2004; Liu et al. 2004; Morlot et al. 2007; Hohenester 2008; Jones et al. 2008).

Compared with Slit2, the biological functions of Slit3 are less explored (Geutskens et al.; Zhang et al. 2009). Genetic studies have observed that Slit3 deficiency leads to a central diaphragmatic hernia and kidney malformation phenotypes in mice (Liu et al. 2003; Yuan et al. 2003), but its underlying mechanisms are not known. Using a recombinant N-terminal fragment of hSlit3, we recently found that Slit3 interacts with Robo4 to promote angiogenesis and suggested that Slit3 deficiency may disrupt developmental angiogenesis in the diaphragm to lead to the central diaphragmatic hernia phenotype in the mutant mice (Zhang et al. 2009). In the current study, we explored the biological function of the hSlit3 C-terminal fragment (HSCF) and observed that HSCF binds heparin and heparan sulfate (HS), but not chondroitin sulfate A (CSA). The binding appeared to be high affinity and depended on the size, the degree of sulfation, the presence of N- and 6-*O*-sulfates and carboxyl moiety of heparin. Functional

[1]To whom correspondence should be addressed: Tel: +1-706-542-6445; Fax: +1-706-542-4412; e-mail: lwang@ccrc.uga.edu

studies observed that HSCF inhibited antithrombin (AT) binding to heparin and neutralized the AT (factor IIa) and antifactor Xa activities of heparin and the antifactor IIa activity of low-molecular-weight heparin (LMWH). HSCF also reversed the anticoagulant activity of heparin in the plasma in the global blood coagulation assay. These observations demonstrate HSCF as a novel heparin-binding protein and reveal a potential for HSCF to be developed as a new antidote to treat overdosing of heparin and LMWH in clinical applications.

Results

Expression of recombinant HSCF

Slit3 has been observed to be cleaved to give rise to N- and C-terminal fragments in vivo (Patel et al. 2001). We recently examined the biological function of a recombinant N-terminal fragment of hSlit3 and observed that the N-terminal fragment potently promotes angiogenesis (Zhang et al. 2009), but the biological function of the C-terminal fragment has not been determined. To explore this issue, we attempted to determine the natural size of the C-terminal fragment initially by transfecting N2A cells with a full-length *hSlit3* expression vector containing an HPC4 tag at the N terminus (Figure 1A). By probing the conditioned medium (CM) from the transfected cells with an anti-HPC4 monoclonal antibody, we detected two bands at ~170 and 120 kDa, respectively (Figure 1B). The 170-kDa band was in agreement with the predicted size of the full-length hSlit3 (167.7 kDa) and the 120-kDa band would correspond to the N-terminal fragment, suggesting that the cleavage of hSlit3 generates an 50-kDa C-terminal fragment. A similar cleavage occurred in hSlit2 and hSlit3 expressed in CHO cells (Patel et al. 2001), and hSlit2 and dSlit expressed in COS and HEK 293 cells (Brose et al. 1999). A putative cleavage site was proposed for hSlit2 (Brose et al. 1999). The sequence of the cleavage site is highly conserved between hSlit2 and hSlit3 (Figure 1C) and two fragments with predicted sizes of 120 kDa (N-terminal) and 50 kDa (C-terminal) would form from this presumed hSlit3 cleavage site, close to the observed size of the C-terminal fragment in our experiment (Figure 1B). Therefore, we designed an HSCF expression construct starting from this presumed cleavage site (Figure 1A) and expressed the construct in N2A and HEK 293 cells (Figure 1B). The recombinant protein was secreted into the CM, purified first on a nickel-nitriloacetic acid (Ni-NTA) column and finally on an anti-HPC4 column. The purified protein ran as a single 50-kDa band on a sodium dodecyl sulfate polyacrylamide gel electrophoresis (SDS-PAGE) gel as predicted (Figure 1B) and was confirmed to be HSCF by mass spectrometry (MS) analysis (Figure 1D). The HSCF appeared as same-sized single bands on SDS–PAGE gels under both reducing and non-reducing conditions (Figure 1E) and as a single peak in gel filtration chromatography (data not shown), indicating that HSCF presents as a monomer in solution.

HSCF binds heparin with high affinity

The Slit2 C-terminal fragment was reported to bind heparin (Hussain et al. 2006). To determine if HSCF also binds to

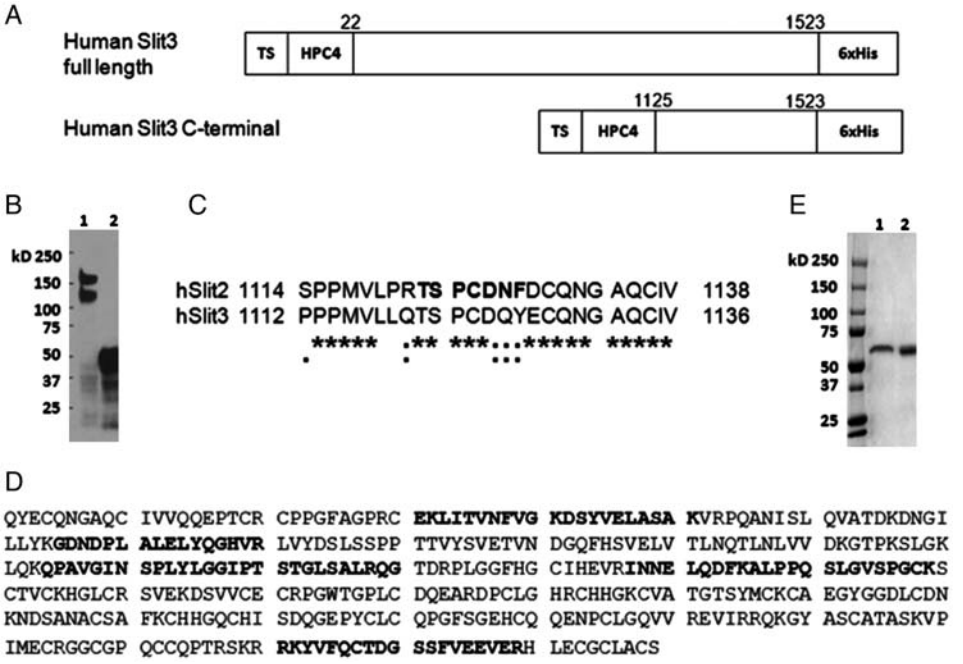

Fig. 1. Expression of recombinant HSCF. (**A**) Schemes of *Slit3* constructs: *Slit3* full length (amino acids 22–1523) and *HSCF* (amino acids 1125–1523). Both constructs have a transferrin signal (TS) peptide followed by an HPC4 tag at the N terminus and a 6× His-tag at the C terminus. (**B**) Slit3 cleavage in vivo. The CMs from N2A cells transfected with full-length (lane 1) and C-terminal (lane 2) hSlit3 containing vector were analyzed by western blot probing with an anti-HPC4 monoclonal antibody. (**C**) Sequence homology between hSlit2 and hSlit3 around the putative cleavage site (bold letters) identified in hSlit*2*. (**D**) MS/MS analysis. Purified HSCF that appeared as a single band on an SDS–PAGE gel was cut out and subjected to MS/MS analysis. Identified peptides are shown in bold letters. (**E**) SDS–PAGE analysis of purified HSCF in reducing (lane 1) and non-reducing conditions (lane 2).

heparin, we injected the purified protein onto a HiTrap Heparin affinity column. HSCF bound to heparin tightly and required a 1.2 M NaCl concentration to elute out from the column (Figure 2A). The binding was alternatively confirmed in enzyme-linked immunosorbent assay (ELISA) and surface plasmon resonance (SPR) analyses. In ELISAs, HSCF was immobilized on 96-well plates and then incubated with various concentrations of biotinylated heparin. Heparin showed a dose-dependent and saturable binding to the immobilized HSCF (Figure 2B). SPR analysis was carried out with heparin immobilized on chip and determined an association rate $k_{on} = 1.29 \times 10^7\ M^{-1}\ s^{-1}$, a dissociation rate $k_{of} = 3.2 \times 10^{-3}\ s^{-1}$ and a binding dissociation constant $K_D = 2.48 \times 10^{-10}$ M (Figure 2C) of the heparin–HSCF interaction, revealing a very high-affinity binding of HSCF to heparin. The sensorgrams were fit with a 1:1 interaction model with mass transfer. The goodness of the fit was indicated by a low χ^2 value (4.22) and suggests that only a single class of high-affinity binding sites is involved in the heparin–HSCF interaction.

HSCF–heparin interaction depends on the degree of sulfation, N- and 6-O-sulfates, carboxyl moiety and size of heparin

To determine whether a specific structure is required for heparin to bind HSCF, we carried out competitive SPR analysis. HSCF was incubated with various concentrations of glycosaminoglycans (GAGs), including heparin, HS and CSA (Table I), and then injected onto a heparin-coated chip and the interactions of HSCF with the immobilized heparin were measured. IC_{50} values were determined as the GAG concentrations that reduced HSCF binding to 50% of the maximal binding (the binding in the absence of GAG). The IC_{50} values for heparin, HS and CSA were determined to be 30 ng/mL, 6.5 µg/mL and 2.2 mg/mL, respectively (Table I). The IC_{50} values demonstrated that HSCF binds heparin and HS, but not CSA, and the binding affinity to heparin was higher than to HS. The structure of heparin is similar to the highly sulfated regions of HS, and the relative number of sulfate groups along the chains in heparin and HS were 2.4 and 0.85

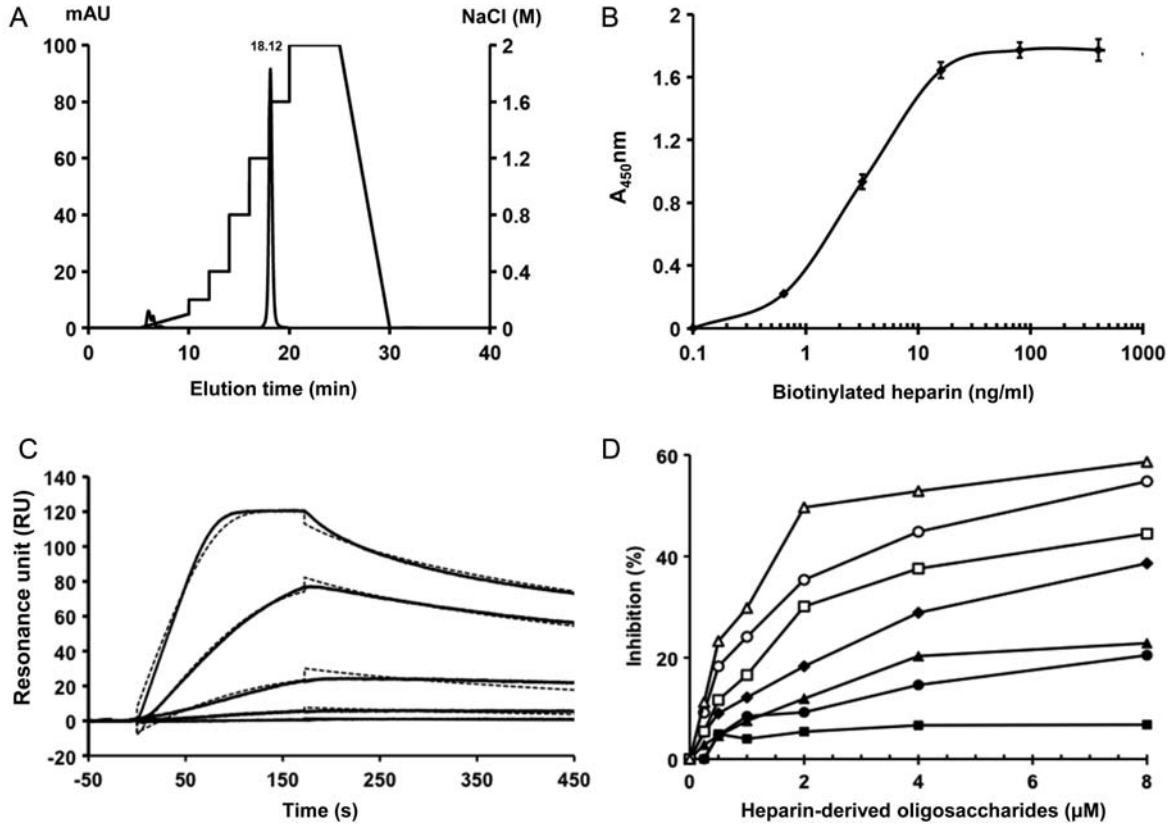

Fig. 2. HSCF binds to heparin with high affinity and depends on size. (**A**) Binding of HSCF to heparin in HPLC analysis. HSCF was applied to a HiTrap Heparin column that was pre-equilibrated in PBS and was eluted with a step gradient of NaCl from 0 to 2 M (dotted line) in PBS at a flow rate of 0.9 mL/min. Chromatogram represents three independent runs. (**B**) Binding of HSCF to heparin in ELISA. Various concentrations of biotinylated heparins were added to HSCF-coated ELISA wells and bound heparin was measured after 2 h incubation. Values are presented as the mean ± SE from three independent runs. (**C**) SPR analysis. Various concentrations of HSCF (6.25, 3.12, 1.56, 0.78 and 0.39 nM from top to bottom) were injected over a heparin-immobilized chip. The response in RU was recorded (solid lines). Fitted curves (dotted lines) were calculated using a 1:1 interaction model with mass transfer. The sensorgram shown is representative of three independent runs. (**D**) Binding of heparin-derived oligosaccharide to HSCF in competitive ELISA. HSCF solutions pre-incubated with heparin-derived oligosaccharides including tetra- (filled squares), hexa- (filled circles), octa- (filled triangles), deca- (filled diamonds), dodeca- (open squares), tetradeca- (open circles) or hexadecasaccharide (open triangles) were added into heparin-coated ELISA wells. After incubation and washing, the HSCF bound was measured. Data are presented as % of inhibition based on the values detected in the absence of oligosaccharides as 0% inhibition. Data are presented as the mean ± SE from three independent experiments.

Table I. Summary of IC_{50} values of HSCF–GAG interactions determined in SPR analysis

Glycosaminoglycan	IC_{50}
Heparin	~30 ng/mL (2 nM)
HS	~6.5 μg/mL
CSA	~2.2 mg/mL
OS-hep	~12.4 ng/mL
2/3-des-hep	~413.9 ng/mL
6-des-hep	~16.39 μg/mL
N-des-hep	~378.5 μg/mL
Carboxyl-reduced heparin	~292.4 μg/mL
LMWH (Enoxaparin)	~288.4 μg/mL
Fondaparinux (Arixtra)	~2633 μg/mL

sulfates/disaccharide, respectively (Schuksz et al. 2008). Thus, this observation revealed a correlation between the binding affinity to the degree of sulfation of heparin. However, the similarly tested CSA, which has a comparable degree of sulfation (0.95 sulfates/disaccharide) to HS (Schuksz et al. 2008), showed a much higher IC_{50} than that of HS, suggesting the existence of heparin/HS-specific structures that are necessary for HSCF binding. This was further examined using several chemically modified heparins. Compared with heparin, the oversulfated heparin (OS-hep) showed a slightly higher binding affinity than heparin with an IC_{50} of 12.4 ng/mL, whereas all the desulfated heparins exhibited reduced binding affinities following the order: 2-/3-*O*-desulfated heparin (2/3-des-hep; IC_{50} = 413.9 ng/mL) ≫ > 6-des-hep (6-*O*-desulfated heparin; IC_{50} = 16.3 μg/mL) > *N*-des-hep (*N*-desulfated/*N*-acetylated heparin; IC_{50} = 378.5 μg/mL) (Table I). These observations further supported that the HSCF binding depends on the degree of sulfation and also revealed the particular importance of N- and 6-*O*-sulfate groups in the binding. In addition, carboxyl-reduced heparin (CR-hep) showed a very low binding affinity for HSCF with an IC_{50} of 292.4 μg/mL (Table I), indicating that the carboxyl groups are critically required for the binding also. Taken together, these observations demonstrated that the HSCF–heparin interaction critically depends on both the degree of sulfation and heparin/HS-specific modifications. Among the specific modifications, N- and 6-*O*-sulfation and carboxylation are essential for the binding.

To determine the size required for heparin to bind HSCF, the protein was incubated with heparin-derived oligosaccharides ranging from tetrasaccharide to hexadecasaccharide in heparin-coated ELISA wells. After washing, the HSCF bound on the wells was measured. Except tetrasaccharides, all other oligosaccharides showed significant and dose-dependent inhibitions on binding of HSCF to immobilized heparin (Figure 2D). Among the inhibitory oligosaccharides, hexasaccharides was the smallest, suggesting that an oligosaccharide with 6-sugar residues is the minimal size required for HSCF binding. Meanwhile, comparison among the inhibitory oligosaccharides observed that the inhibitory potencies positively correlated with their sizes, indicating that the high-affinity binding of HSCF requires a size larger than a hexasaccharide. This prospection was strongly supported by examining the interaction of HSCF with the LMWH enoxaparin (average MW at 4500 Da, equivalent to 16-mer heparin oligosaccharide) and fondaparinux, a heparin-containing pentasaccharide with N- and 6-*O*-sulfation and carboxylation, in SPR analysis. We observed that enoxaparin, but not Arixtra, inhibited the binding of HSCF to immobilized heparin in SPR analysis (Table I), further demonstrating the critical size of heparin for interaction with HSCF. Combined with our aforementioned observation that HSCF potently inhibited AT binding to heparin, we suggest that the binding site for HSCF in heparin is a hexamer or a larger oligosaccharide containing or adjacent to the AT-binding site.

HSCF neutralizes the antifactor IIa and Xa activities of heparin, and antifactor Xa activity of LMWH

Heparin is a commonly used anticoagulant in clinical settings and exerts its anticoagulant activity by binding AT, thereby enhancing AT's inhibitory effect on coagulation proteases, especially factors Xa and IIa and to some extent factors IXa, XIa and XIIa (Rosenberg and Damus 1973; Björk and Lindahl 1982; Rosenberg and Rosenberg 1984). Structural analysis revealed that the enhanced inhibition on factor Xa only requires AT binding to a specific pentasaccharide sequence in heparin (the AT-binding site; Lindahl et al. 1979; Petitou et al. 2003), whereas the increased inactivation of factor IIa occurs only when AT and factor IIa bind together to a longer heparin chain of at least 18 saccharides (Lane et al. 1984). The high-affinity binding of HSCF to heparin led us to test whether it can block AT binding to heparin, thereby neutralizing the antifactor IIa and Xa activities of heparin. To test this hypothesis, we first examined if HSCF was able to compete with AT in heparin binding. We observed that HSCF dose-dependently inhibited AT binding to immobilized heparin with a calculated apparent IC_{50} of 4.7 nM and a maximum inhibition of ~60% (Figure 3A). This indicates that HSCF potently inhibited AT binding to heparin. To determine whether the inhibitory effect of HSCF on AT binding could affect the anticoagulant activity of heparin, we carried out antifactor IIa and Xa amidolytic assays. HSCF dose-dependently and potently inhibited the inactivation of factors IIa and Xa by AT (Figure 3B and C). For example, HSCF at 1.5 μM completely inhibited the thrombin inactivation and inhibited 80% factor Xa inactivation at 2.5 μM. In the SPR assay, HSCF was observed to bind to LMWH enoxaparin, but not to fondaparinux, we therefore further examined whether HSCF could inhibit their antifactor Xa activities. As shown in Figure 3C, HSCF inhibited enoxaparin- but not fondaparinux-mediated inactivation of factor Xa. These results demonstrated that that HSCF neutralized the antifactor IIa and Xa activities of heparin, and antifactor Xa activity of LMWH, but not of fondaparinux.

HSCF reverses the prolongation of plasma clotting time produced by heparin

To test whether the neutralizing effect of HSCF on heparin observed in antifactor IIa and Xa chromogenic assays is relevant in the global blood coagulation, thromboelastography (TEG) assay was performed using citrated pooled plasma. TEG has been used increasingly for monitoring the administration of heparin, LMWH and heparinoids in patients (Bolliger et al. 2012; van Geffen and van Heerde 2012). TEG

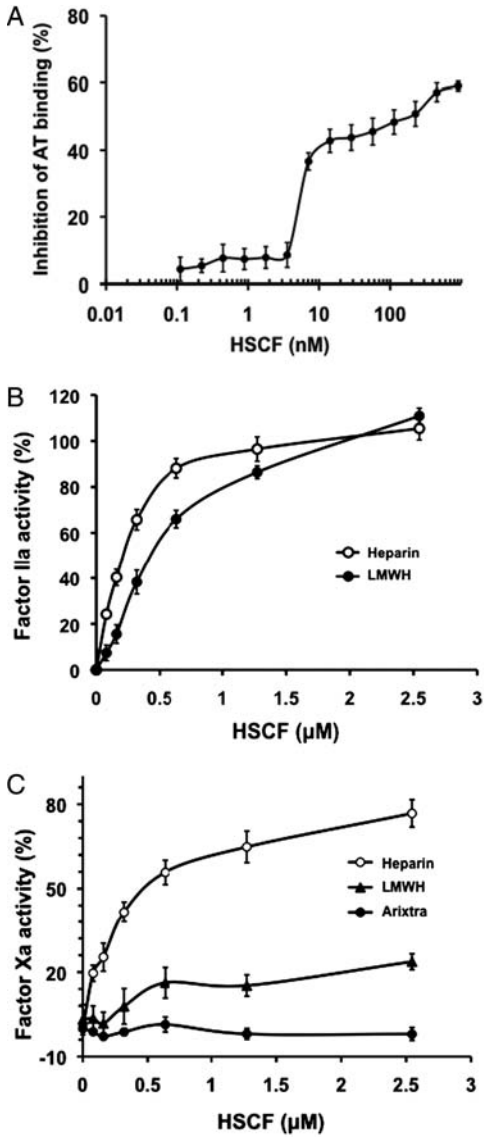

Fig. 3. HSCF inhibits AT binding to heparin and neutralizes the antifactor IIa and/or Xa activity of heparin and LWMH, but not of Arixtra. (**A**) HSCF inhibited AT binding to heparin. AT (50 ng/mL) premixed with various concentrations of HSCF was added to heparin-immobilized ELISA wells and bound AT was measured after incubation. Points are presented as % of inhibition compared with values detected in the absence of HSCF as 0% inhibition. Data are presented as the mean ± SE from three independent experiments. (**B**) HSCF neutralizes the antifactor IIa activity of heparin and LMWH. Unfractionated heparin (open circles) or enoxaparin (filled circles) were incubated with AT, thrombin and various concentrations of HSCF, and then the chromogenic substrate S-2238 was added. Residual thrombin activity was quantified by measuring the absorbance at 405 nm. The antifactor IIa activity in the absence of heparin or LMWM was defined as 100%. The data are presented as the mean ± SE from three independent measurements. (**C**) HSCF neutralizes the antifactor Xa activity of heparin and LMWH, but not of fondaparinux. Unfractionated heparin (open circles), enoxaparin (filled triangles) or fondaparinux (filled circles) were incubated with AT, factor Xa and various concentrations of HSCF, and then the chromogenic substrate S-2222 was added. Residual factor Xa was quantified by measuring the absorbance at 405 nm. The factor Xa activity in the absence of GAGs was defined as 100%. The data are presented as the mean ± SE from three independent measurements.

measures the dynamic process of blood coagulation with defined parameters reflecting the integrity of hemostatic components, including the time a detectable clot is formed (R), the rate of clot formation (Ang) and clot strength (maximal amplitude, MA; Figure 4A). The smaller the R and the larger the Ang and MA values, the greater the coagulability of the blood is. In our study, the test was terminated when those values appeared on the TEG recordings. However, when there were no values given because the blood samples could not form a clot, the test was terminated at 60 min. In the latter cases, values of 60 min for R and zero for both Ang and MA were assigned arbitrarily. With these values, the efficacy of HSCF for reversing the anticoagulant effect of heparin was determined in the plasma with or without kaolin, a strong activator of the intrinsic coagulation pathway.

We first examined the effect on coagulation without kaolin. As shown in Figure 4B and D, the pooled citrated plasma had an R value of 10.60 ± 1.47 min, an Ang value of 21.83 ± 3.51 and an MA value of 13.70 ± 1.04. Addition of heparin (0.1 U/mL) completely inhibited plasma coagulation, showing an *R*-value >60 min, whereas the addition of HSCF at 50 μg/mL (1 μM) reversed the heparin inhibition and restored the plasma to coagulate, reaching an *R* time of 13.70 ± 1.04 min. We further examined the effect of HSCF on heparinized plasma with coagulation activated by kaolin. Kaolin significantly accelerated the coagulation of the citrated plasma, resulting in a shorter *R*-value (4.17 ± 0.19 min). The kaolin addition also coagulated the heparinized plasma (heparin at 0.1 U/mL), but showed a prolonged R time (5.80 ± 0.40 min). Addition of HSCF (50 μg/mL) shortened the heparin-prolonged R time to 4.85 ± 0.25 min. The inhibitory effect of HSCF on heparin anticoagulation of the plasma was also reflected by the increasing values of Ang and MA upon HSCF addition (Figure 4B–D). Therefore, under both non-activated and kaolin-activated conditions, HSCF reversed the prolongation of blood coagulation produced by heparin.

Discussion

In this study, we present evidence for the first time showing that HSCF is a novel, high-affinity heparin-binding protein. Heparin exerts its biological functions mainly by ionic interactions with proteins (Capila and Linhardt 2002; Esko et al. 2009). In some cases, like the interactions with fibronectin (Ogamo et al. 1985) and platelet factor 4 (Maccarana and Lindahl 1993), the strength of the binding depends more on the length and degree of sulfation and less on a specific sequence. In other cases, the binding sites correspond to short oligosaccharide stretches with defined sequences: examples include the AT-binding site (Petitou et al. 2003), vascular endothelial growth factor (VEGF) binding site (Robinson et al. 2006) and FGF-binding site (Maccarana et al. 1993). In our study, we observed that the high-affinity binding of HSCF depends on the degree of sulfation, N- and 6-*O*-sulfate and carboxyl groups of heparin. We also observed that the binding requires a minimal size of 6-sugar residues and the larger heparin-derived oligosaccharide showed higher binding affinities. It is interesting to note that HSCF potently inhibited binding of AT to heparin. This observation suggested that the

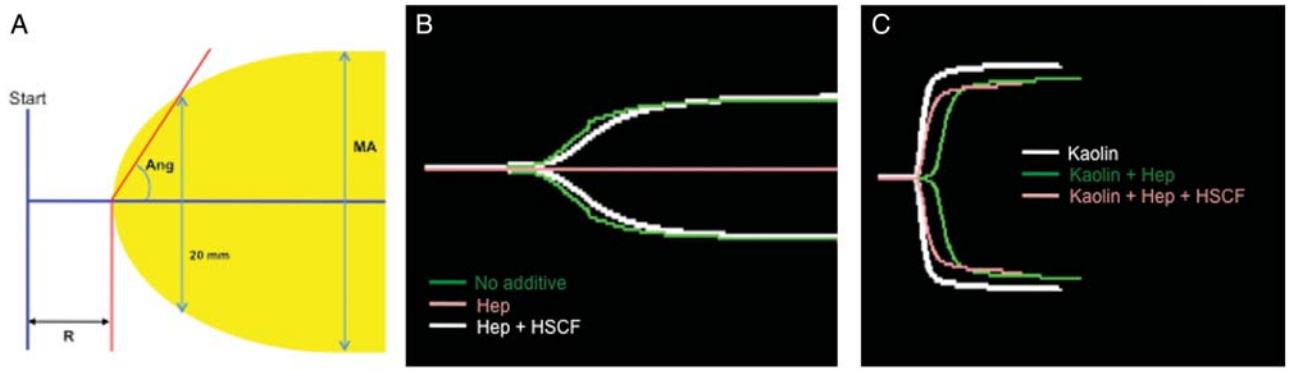

D

	− kaolin			+ kaolin		
	R (min)	Ang	MA	R	Ang	MA
No additive	10.60 ± 1.47	21.83 ± 3.51	13.70 ± 1.04	4.17 ± 0.19	73.60 ± 1.06	21.55 ± 0.20
Heparin	> 60	0	0	5.80 ± 0.40	57.55 ± 2.95	19.15 ± 0.05
Heparin + HSCF	13.7 ± 1.04#	13.85 ± 2.25#	11.85 ± 0.05#	4.85 ± 0.25*	65.50 ± 0.90*	18.90 ± 1.00

Fig. 4. HSCF reverses the prolongation of blood coagulation produced by heparin in TEG assay. (**A**) A normal TEG scheme showing the R, Ang and MA parameters. R, the time a detectable clot is formed; Ang, the rate of clot formation; MA, clot strength. (**B**) TEG of non-koalin-activated coagulation of plasma in the absence or the presence of heparin without/with HSCF. (**C**) TEG of koalin-activated plasma coagulation in the absence or the presence of heparin without/with HSCF. (**D**) Summary of the parameters measured in (B) and (C). The data are presented as the mean ± SEM, $n = 3$. The significance of the difference between heparin and heparin + HSCF groups was analyzed by paired Student's *t*-test. #$P < 0.001$ (non-koalin-activated samples) and *$P < 0.05$ (koalin-activated samples).

AT-binding site in heparin is involved in HSCF binding. However, we also observed that HSCS does not bind fondaparinux, the unique pentasaccharide high-affinity AT-binding site in heparin. Based on these observations we propose that the minimal binding site for HSCF is a 6-mer heparin sequence with N- and 6-*O*-sulfates, and in heparin, the minimal binding site for HSCF may contain or be adjacent to the AT-binding site. The precise sequence of the HSCF-binding site in heparin needs to be further determined.

Heparin and LMWH are commonly applied to prevent or treat thromboembolic disorders and to prevent clotting of extracorporeal blood during hemodialysis and cardiac surgery (Kessler 2004). As with every anticoagulant, heparin and LMWH are associated with bleeding risks (Crowther and Warkentin 2008). Protamine sulfate has been used clinically to reverse the bleeding caused by heparin and LMWH overdosing (Crowther and Warkentin 2008). However, protamine sulfate is a non-specific heparin/LMWH inhibitor and can have serious side effects like anaphylactic and anafilactoid reactions that in some cases can be fatal (Crowther and Warkentin 2008; Nybo and Madsen 2008). Thus, a safer and effective antidote to heparin/LMWH is needed. HSCF potently inhibited the binding of AT to heparin and LMWH and neutralized their anticoagulant activities, showing that HSCF can function as an effective antidote to heparin and LMWH. Meanwhile, HSCF is a natural protein fragment in human and is unlikely to induce the anafilactic reactions that can caused by protamine sulfate in patients. Therefore, HSCF has the potential to be developed as an effective and safer antidote toward heparin and LMWH overdosing in clinical applications.

Several high-affinity heparin-binding proteins, including serum amyloid P component and platelet factor 4, have been shown to effectively neutralize the anticoagulant activity of heparin, whereas the others, such as vitronectin and histidine-rich glycoprotein, have very weak or no neutralization effect (Williams et al. 1992). The neutralization capacity of these heparin-binding proteins appears not to solely depend on their binding affinity to heparin, as evidenced that vitronectin ($Kd = 10^{-2}$ μM) and histidine-rich glycoprotein ($Kd = 7 \times 10^{-2}$ μM) have higher binding affinity to heparin than the serum amyloid P compenent ($Kd = 1.5$ μM) and platelet factor 4 ($Kd = 3 \times 10^{-2}$ μM) (Li et al. 1994; Conrad 1998). These observations indicate that the antidote effect of HSCF to heparin is not unique among heparin-binding proteins and the heparin neutralization effect is not a general feature for heparin-binding proteins.

In mammals, heparin is only produced in mast cells in connective tissues (Bishop et al. 2007), whereas HS, which contains heparin-like structures, is ubiquitously expressed on the cell surfaces and in the extracellular matrix of all tissues. HS critically modulates the biological functions of cytokines, chemokines, growth factors, morphogens, proteases and protease inhibitors through several mechanisms, including serving as a

depot to store and to protect the protein ligands from degradation, facilitating the formation of morphogen gradients essential for cell specification and migration and co-receptor functions (Bishop et al. 2007; Fuster and Wang). Slit3 is a secreted protein and functions to induce cell migration and proliferation by interacting with its receptor Robo4 (Geutskens et al.; Zhang et al. 2009). In this study, HSCF has been shown to bind both heparin and HS. We also observed that the N-terminal of Slit3 binds heparin (Zhang et al. manuscript in preparation). Therefore, it appears that full-length Slit3 possesses two HS-binding sites, which resides in the N- and C-terminal fragments, respectively. Interestingly, previous studies by others have also observed that the C- and N-terminal fragments of Slit2 both bind heparin and HS (Hu 2001; Ronca et al. 2001; Zhang et al. 2004), suggesting that the two HS-binding sites in Slit proteins are conserved. The HS-binding characteristic also suggests that the full-length Slit protein may interact with HS to maintain a gradient in the extracellular matrix to direct cell migration and to facilitate Slit-Robo engagement on the cell surface. Meanwhile, the naturally generated N- and C-terminal fragment through cleavage, each having its own HS-binding site, may compete with the full-length Slit protein for HS binding to disrupt the gradient formation and the co-receptor function. Therefore, this HS-based competition may represent a general, negative feedback and fine regulatory mechanism of the Slit signaling in nature. In addition, similar to the competitive inhibition of AT binding to heparin, full-length Slits and their N- and C-terminal fragments may compete with cytokines, chemokines, growth factors and morphogens for HS binding to modulate these protein ligand-mediated, HS-dependent physiological and pathological functions. Therefore, the interaction with HS may also represent a general mechanism for Slits to crosstalk with other HS-binding proteins.

Materials and methods

GAG and heparin-derived oligosaccharide

Porcine intestinal heparin (Mw = 12,000–15,000 Da) was obtained from Scientific Protein Laboratories (Waunakee, WI). Heparinoids were prepared as previously reported, including OS-hep, *N*-des-hep, 2/3-des-hep, 6-des-hep and CR-hep (Wang et al. 2002; Zhang et al.). Biotinylated heparin was prepared with biotin coupled at heparin's reducing end (Osmond et al. 2002; Zhang et al.). HS and CSA were purchased from Sigma-Aldrich (St Louis, MO). Enoxaparin was purchased from Sanofi-Aventis (Bridgewater, NJ). Enoxaparin is a clinically widely used LMWH with an average molecular weight of 4500 Da (equivalent to a 16-oligosaccharide chain). Its actual size distribution includes ~74% of the oligosaccharide chains with a molecular weight between 2000 and 8000 Da, ~16% with a molecular weight lower than 2000 Da and ~18% of the chains with a molecular weight higher than 8000 Da. Fondaparinux (methyl-*O*-2-deoxy-6-*O*-sulfo-2-(sulfoamino)-α-D-glucopyranosyl-(1 → 4)-*O*-β-D-glucopyranuronosyl-(1 → 4)-*O*-2-deoxy-3,6-di-*O*-sulfo-2-(sulfoamino)-α-D-glucopyranosyl-(1 → 4)-*O*-2-*O*-sulfo-α-L-idopyranuronosyl-(1 → 4)-2-deoxy-6-*O*-sulfo-2-(sulfoamino)-α-D-glucopyranoside, decasodium salt) was purchased from GlaxoSmithKline (Brentford, UK). Heparin-derived oligosaccharides were prepared by partial digestion with heparinase I (Grampyan Enzymes, Orkney, UK) and fractionated on a high-performance liquid chromatography (HPLC) Sephacryl S-100 column (3.2 cm ID × 100 cm). Each fraction was further purified on a TSKGel G3000SWXL column (7.8 mm ID × 30 cm) connected in series with a TSKGel G2000SWXL column (7.8 mm ID × 30 cm) (Tosoh Bioscience, King of Prussia, PA; Rice et al. 1985). The fractions corresponding to tetrasaccharide to decasaccharide were confirmed by electrospray ionization mass spectrometry analysis.

Expression and purification of HSCF

Full-length and a C-terminal fragment (amino acids 1123–1523) of *hSlit3* were cloned into pcDNA 3.1 vector (Invitrogen, Carlsbad, CA) containing a transferrin signal peptide followed by an HPC4 epitope (Rezaie and Esmon 1992) at the N terminus and a 6× His-tag at the C terminus. The expression vectors were transfected into mouse neuroblastoma cells N2A (ATTC, Manassas, VA) and stable colonies expressing HSCF were selected after screening CMs with an anti-HPC4 antibody (Roche Applied Science, Mannheim, Germany) in western blot analysis. Stable cell clones expressing HSCF were cultured in Dulbecco's Modified Eagle Medium (Hyclone, Logan, UT) with N2 NeuroPlex serum-free supplement (Gemini Bio-Products, West Sacramento, CA). Alternatively, for large-scale production of HSCF, the expression vector was transiently transfected into suspension-adapted HEK293 cells. In both cases, CM was collected after 5 days and recombinant protein was purified passing through a Ni-NTA column (Qiagen, Valencia, CA) and an anti-HPC4 antibody-conjugated Affi-gel 10 column (Rezaie and Esmon 1992). The purified protein was partially sequenced by liquid chromatography-mass spectrometry/mass spectrometry analysis and was confirmed to be HSCF.

Heparin affinity chromatography

Fifteen micrograms of HSCF was injected onto a 1-mL HiTrap Heparin column (GE Healthcare, Piscataway, NJ) that was pre-equilibrated with phosphate buffered saline (PBS), pH 7.4, and coupled to an Agilent 1200 HPLC system (Agilent Technologies, Palo Alto, CA). The protein was eluted with a step gradient of NaCl from 0 to 2 M in PBS, pH 7.4, at a 0.9-mL/min flow rate and monitored for absorbance at 280 nm.

Enzyme-linked immunosorbent assays

Binding of heparin to immobilized HSCF. HSCF at 400 ng/mL in Tris-buffered saline (TBS, 10 mM Tris–HCl, pH 7.4, 150 mM NaCl) was added to 96-well ELISA plates and incubated for 2 h at room temperature (RT). After washing and blocking with TBST (TBS with 0.05% Tween-20) plus 3% BSA, biotinylated heparin was added in various concentrations and incubated for 2 h at RT. Bound heparin was detected after incubation with streptavidin-horseradish peroxidase (HRP) and 3,3′,5,5′-tetramethylbenzidine (TMB) chromogen (Thermo Fisher, San Jose, CA).

Inhibition of HSCF binding to heparin. Heparin-coated wells were prepared by incubating biotinylated heparin at 50 μg/mL in TBST, 0.1% BSA on streptavidin-conjugated 96-well plates (Pierce Biotechnology, Rockford, IL) for 2 h. After washing, the wells were incubated for 2 h at RT with HSCF that was pre-mixed with various concentrations of GAGs. Bound HSCF was detected by sequential incubation with an anti-HPC4 antibody, an HRP-conjugated secondary antibody and TMB.

Inhibition of AT binding to heparin by HSCF. Human AT (Sigma-Aldrich) pre-mixed with various concentrations of HSCF was added to the heparin-coated ELISA wells and incubated for 2 h at RT. Bound AT was detected with an antihuman AT antibody (Sigma-Aldrich) as the primary antibody.

SPR analysis

SPR experiments were performed on a Biacore T100 instrument (GE Healthcare). Streptavidin was covalently attached to the surface of a CM5 chip (GE Healthcare) using the amine coupling method (Amara et al. 1999; Osmond et al. 2002) and the remaining activated groups were blocked by ethanolamine injection. Biotinylated heparin was then injected to give ~1000 response units (RU). One flow cell of the chip was used as a control for background subtraction having only streptavidin immobilized on the chip. For kinetic studies, a series of concentrations of HSCF in HBS-T buffer {10 mM 4-(2-hydroxyethyl)-1-piperazineethanesulfonic acid, pH 7.4, 150 mM NaCl, 0.005% v/v Tween-20} was injected on the chip for 180 s with a flow rate of 30 μL/min. A dissociation time of 240 s was set up followed by regeneration with 2 M NaCl in HBS-T buffer. Kinetic parameters were calculated with the Biacore T100 Evaluation software using a 1:1 binding model. For the solution competition studies, HSCF at a final concentration of 5 nM was mixed with various concentrations of GAGs and then immediately injected. The effect of GAGs on the binding of HSCF to immobilized heparin was monitored as relative RU that was used to calculate IC_{50} values with the GraphPad Prism software (GraphPad Software, San Diego, CA).

Antifactor Xa assay

A chromogenic antifactor Xa assay was carried out using a Coatest heparin kit (Chromogenix, Bedford, MA) according to the manufacturer's instructions adapted to a 96-well plate format. In brief, samples (80 μL) containing 8 μL of human normal plasma in 50 mM Tris, pH 8.5, were incubated for 3 min at 37°C with human AT (0.1 IU/mL) in the absence or the presence of heparin (30 mIU/mL), enoxaparin (250 ng/mL) or fondaparinux (30 ng/mL) and various concentrations of HSCF, and then 40 μL of bovine factor Xa (7.1 nkat/mL) were added and incubated for 30 s at 37°C. The residual factor Xa activity was determined after incubation with 80 μL of substrate S-2222 (1 mM) for 3 min at 37°C, stopping the reaction with 60 μL of acetic acid 20% and measuring the change of absorbance at 405 nm.

Antifactor IIa assay

Antifactor IIa (thrombin) activity was measured using a heparin anti-IIa kit (Diapharma Group, West Chester, OH) according to the manufacturer's instructions adapted to a 96-well plate format. Briefly, samples (50 μL) containing various concentrations of HSCF in 50 mM Tris, pH 8.5, 150 mM NaCl, 2 mg/mL bovine serum albumin were pre-incubated for 4 min at 37°C in the presence or the absence of heparin (5 mIU/mL) or enoxaparin (200 ng/mL), and subsequently, 50 μL of human AT (0.31 IU/mL) was added and then incubated for another 2 min at 37°C. Following, 50 μL of human thrombin (5 NIH units/mL) was added and incubated for 90 s. The residual thrombin activity was determined after incubation with 50 μL of substrate S-2238 (0.78 mg/mL) for 3 min at 37°C, stopping the reaction with 50 μL of acetic acid 20% and measuring the change of absorbance at 405 nm.

Thromboelastography

TEG was performed on a TEG-5000 instrument (Haemonetics, Braintree, MA) according to the manufacturer's instructions (Pittman et al. 2010). All disposable supplies were purchased from Haemonetics. Briefly, 20 μL of 0.2 M $CaCl_2$ was added to a disposable TEG cup pre-warmed at 37°C. To this cup, 340 μL of pooled, citrated plasma that had been pre-incubated for 5 min with a number of different additives was added. Additives to the plasma (shown at final concentrations in the cup) included: unfractionated heparin at 0.1 U/mL only, unfractionated heparin at 0.1 U/mL + HSCF at 50 μg/mL, or HSCF at 50 μg/mL only. Control plasma samples with no additives were also evaluated. For kaolin-activated samples, 5 μL of kaolin solution (Haemonetics) was added to the plasma samples immediately prior to the initiation of the assay; the sample was mixed by pipette aspiration five times, and then was added to the warmed TEG cup. TEG parameters measured included R time in minutes, representing the time until initial fibrin formation was detected in the sample, angle, measured in degrees and representing the rate of clot formation, and MA, measured in mm and representing the final clot strength. All assays were allowed to run for 60 min or until generation of all three values.

Funding

This work was supported by grants from NIH R01HL093339 (L.W.) and RR005351/GM103390 (L.W. and K.M.) and a grant from National Natural Science Foundation of China #81000196 (L.W.).

Acknowledgement

We appreciate Ms Karen Howard for her English revision of the manuscript.

Conflict of interest

The authors indicate no potential conflicts of interest.

Abbreviations

AT, antithrombin; CM, conditioned medium; CHO, Chinese harmster ovary; CR-hep, carboxyl-reduced heparin; CSA, chondroitin sulfate A; 2/3-des-hep, 2-/3-*O*-desulfated heparin; 6-des-hep, 6-*O*-desulfated heparin; dSlit, *Drosophila* Slit; EGF, epidermal growth factor; GAG, glycosaminoglycan; HEK, Human Embryonic Kidney; HPLC, High-performance liquid chromatography; HRP, horseradish peroxidase; HS, heparan sulfate; HSCF, human Slit3 C-terminal fragment; hSlit, human Slit; LMWH, low-molecular-weight heparin; MA, maximal amplitude; MS, Mass Spectrometry; *N*-des-hep, *N*-desulfated/*N*-acetylated heparin; Ni-NTA, nickel-nitriloacetic acid; OS-hep, oversulfated heparin; PBS, phosphate buffered saline; RT, room temperature; RU, response units; SDS-PAGE, Sodium dodecyl sulfate polyacrylamide gel electrophoresis; SPR, surface plasmon resonance; TBS, Tris-buffered saline; TBST, TBS with 0.05% Tween-20; TEG, thromboelastography; TMB, 3,3′,5,5′-tetramethylbenzidine.

References

Amara A, Lorthioir O, Valenzuela A, Magerus A, Thelen M, Montes M, Virelizier JL, Delepierre M, Baleux F, Lortat-Jacob H, et al. 1999. Stromal cell-derived factor-1alpha associates with heparan sulfates through the first beta-strand of the chemokine. *J Biol Chem*. 274:23916–23925.

Bishop JR, Schuksz M, Esko JD. 2007. Heparan sulphate proteoglycans fine-tune mammalian physiology. *Nature*. 446:1030–1037.

Björk I, Lindahl U. 1982. Mechanism of the anticoagulant action of heparin. *Mol Cell Biochem*. 48:161–182.

Bolliger D, Seeberger MD, Tanaka KA. 2012. Principles and practice of thromboelastography in clinical coagulation management and transfusion practice. *Transfus Med Rev*. 26:1–13.

Brose K, Bland KS, Wang KH, Arnott D, Henzel W, Goodman CS, Tessier-Lavigne M, Kidd T. 1999. Slit proteins bind Robo receptors and have an evolutionarily conserved role in repulsive axon guidance. *Cell*. 96:795–806.

Capila I, Linhardt RJ. 2002. Heparin-protein interactions. *Angew Chem Int Ed Engl*. 41:391–412.

Conrad HE. 1998. *Heparin-Binding Proteins*. San Diego: Academic Press.

Crowther MA, Warkentin TE. 2008. Bleeding risk and the management of bleeding complications in patients undergoing anticoagulant therapy: Focus on new anticoagulant agents. *Blood*. 111:4871–4879.

Esko JD, Kimata K, Lindahl U. 2009. *Proteoglycans and sulfated glycosaminoglycans*. In: Varki A, Cummings RD, et al. editors. *Essentials of Glycobiology*, 2nd edition. Cold Spring Harbor (NY): Cold Spring Harbor Laboratory Press. P. 229–248.

Fuster MM, Wang L. 2010. Endothelial heparan sulfate in angiogenesis. *Prog Mol Biol Transl Sci*. 93:179–212.

Geutskens SB, Hordijk PL, van Hennik PB. 2010. The chemorepellent Slit3 promotes monocyte migration. *J Immunol*. 185:7691–7698.

Hohenester E. 2008. Structural insight into Slit-Robo signalling. *Biochem Soc Trans*. 36:251–256.

Howitt JA, Clout NJ, Hohenester E. 2004. Binding site for Robo receptors revealed by dissection of the leucine-rich repeat region of Slit. *EMBO J*. 23:4406–4412.

Hu H. 2001. Cell-surface heparan sulfate is involved in the repulsive guidance activities of Slit2 protein. *Nat Neurosci*. 4:695–701.

Hussain SA, Piper M, Fukuhara N, Strochlic L, Cho G, Howitt JA, Ahmed Y, Powell AK, Turnbull JE, Holt CE, et al. 2006. A molecular mechanism for the heparan sulfate dependence of slit-robo signaling. *J Biol Chem*. 281:39693–39698.

Itoh A, Miyabayashi T, Ohno M, Sakano S. 1998. Cloning and expressions of three mammalian homologues of *Drosophila* slit suggest possible roles for Slit in the formation and maintenance of the nervous system. *Brain Res Mol Brain Res*. 62:175–186.

Jones CA, London NR, Chen H, Park KW, Sauvaget D, Stockton RA, Wythe JD, Suh W, Larrieu-Lahargue F, Mukouyama YS, et al. 2008. Robo4 stabilizes the vascular network by inhibiting pathologic angiogenesis and endothelial hyperpermeability. *Nat Med*. 14:448–453.

Kessler CM. 2004. Current and future challenges of antithrombotic agents and anticoagulants: Strategies for reversal of hemorrhagic complications. *Semin Hematol*. 41:44–50.

Lane DA, Denton J, Flynn AM, Thunberg L, Lindahl U. 1984. Anticoagulant activities of heparin oligosaccharides and their neutralization by platelet factor 4. *Biochem J*. 218:725–732.

Li XA, Hatanaka K, Guo L, Kitamura Y, Yamamoto A. 1994. Binding of serum amyloid P component to heparin in human serum. *Biochim Biophys Acta*. 1201:143–148.

Lindahl U, Backstrom G, Hook M, Thunberg L, Fransson LA, Linker A. 1979. Structure of the antithrombin-binding site in heparin. *Proc Natl Acad Sci USA*. 76:3198–3202.

Liu Z, Patel K, Schmidt H, Andrews W, Pini A, Sundaresan V. 2004. Extracellular Ig domains 1 and 2 of Robo are important for ligand (Slit) binding. *Mol Cell Neurosci*. 26:232–240.

Liu J, Zhang L, Wang D, Shen H, Jiang M, Mei P, Hayden PS, Sedor JR, Hu H. 2003. Congenital diaphragmatic hernia, kidney agenesis and cardiac defects associated with Slit3-deficiency in mice. *Mech Dev*. 120:1059–1070.

Maccarana M, Casu B, Lindahl U. 1993. Minimal sequence in heparin/heparan sulfate required for binding of basic fibroblast growth factor. *J Biol Chem*. 268:23898–23905.

Maccarana M, Lindahl U. 1993. Mode of interaction between platelet factor 4 and heparin. *Glycobiology*. 3:271–277.

Morlot C, Thielens NM, Ravelli RB, Hemrika W, Romijn RA, Gros P, Cusack S, McCarthy AA. 2007. Structural insights into the Slit-Robo complex. *Proc Natl Acad Sci USA*. 104:14923–14928.

Nybo M, Madsen JS. 2008. Serious anaphylactic reactions due to protamine sulfate: A systematic literature review. *Basic Clin Pharmacol Toxicol*. 103:192–196.

Ogamo A, Nagai A, Nagasawa K. 1985. Binding of heparin fractions and other polysulfated polysaccharides to plasma fibronectin: Effects of molecular size and degree of sulfation of polysaccharides. *Biochim Biophys Acta Gen Subj*. 841:30–41.

Osmond RI, Kett WC, Skett SE, Coombe DR. 2002. Protein-heparin interactions measured by BIAcore 2000 are affected by the method of heparin immobilization. *Anal Biochem*. 310:199–207.

Patel K, Nash JA, Itoh A, Liu Z, Sundaresan V, Pini A. 2001. Slit proteins are not dominant chemorepellents for olfactory tract and spinal motor axons. *Development*. 128:5031–5037.

Petitou M, Casu B, Lindahl U. 2003. 1976–1983, a critical period in the history of heparin: The discovery of the antithrombin binding site. *Biochimie*. 85:83–89.

Pittman JR, Koenig A, Brainard BM. 2010. The effect of unfractionated heparin on thromboelastographic analysis in healthy dogs. *J Vet Emerg Crit Care*. 20:216–223.

Rezaie AR, Esmon CT. 1992. The function of calcium in protein-C activation by thrombin and the thrombin-thrombomodulin complex can be distinguished by mutational analysis of protein-C derivatives. *J Biol Chem*. 267:26104–26109.

Rice KG, Kim YS, Grant AC, Merchant ZM, Linhardt RJ. 1985. High-performance liquid chromatographic separation of heparin-derived oligosaccharides. *Anal Biochem*. 150:325–331.

Robinson CJ, Mulloy B, Gallagher JT, Stringer SE. 2006. VEGF165-binding sites within heparan sulfate encompass two highly sulfated domains and can be liberated by K5 lyase. *J Biol Chem*. 281:1731–1740.

Ronca F, Andersen JS, Paech V, Margolis RU. 2001. Characterization of Slit protein interactions with glypican-1. *J Biol Chem*. 276:29141–29147.

Rosenberg RD, Damus PS. 1973. The purification and mechanism of action of human antithrombin-heparin cofactor. *J Biol Chem*. 248:6490–6505.

Rosenberg RD, Rosenberg JS. 1984. Natural anticoagulant mechanisms. *J Clin Invest*. 74:1–6.

Rothberg JM, Artavanis-Tsakonas S. 1992. Modularity of the slit protein: Characterization of a conserved carboxy-terminal sequence in secreted proteins and a motif implicated in extracellular protein interactions. *J Mol Biol*. 227:367–370.

Rothberg JM, Jacobs JR, Goodman CS, Artavanis-Tsakonas S. 1990. slit: An extracellular protein necessary for development of midline glia and commissural axon pathways contains both EGF and LRR domains. *Genes Dev*. 4:2169–2187.

Schuksz M, Fuster MM, Brown JR, Crawford BE, Ditto DP, Lawrence R, Glass CA, Wang L, Tor Y, Esko JD. 2008. Surfen, a small molecule antagonist of heparan sulfate. *Proc Natl Acad Sci USA*. 105: 13075–13080.

van Geffen M, van Heerde WL. 2012. Global haemostasis assays, from bench to bedside. *Thromb Res*. 129:681–687.

Wang L, Brown JR, Varki A, Esko JD. 2002. Heparin's anti-inflammatory effects require glucosamine 6-O-sulfation and are mediated by blockade of L- and P-selectins. *J Clin Invest*. 110:127–136.

Williams EC, Huppert BJ, Asakura S. 1992. Neutralization of the anticoagulant effects of glycosaminoglycans by serum amyloid P component: Comparison with other plasma and platelet proteins. *J Lab Clin Med*. 120:159–167.

Yuan W, Rao Y, Babiuk RP, Greer JJ, Wu JY, Ornitz DM. 2003. A genetic model for a central (septum transversum) congenital diaphragmatic hernia in mice lacking Slit3. *Proc Natl Acad Sci USA*. 100:5217–5222.

Zhang S, Condac E, Geng JG, Bicknell R, Esko JD, Wang L. Heparin-induced leukocytosis requires 6-O-sulfation and is caused by blockade of selectin- and CXCL12-mediated leukocyte trafficking in mice. *J Biol Chem*.

Zhang B, Dietrich UM, Linhardt RJ, Margolis RU. 2009. Repulsive axon guidance molecule Slit3 is a novel angiogenic factor. *Blood*. 114:4300–4309.

Zhang F, Ronca F, Qiu H, Jiang J, Gutierrez-Sanchez G, Bergmann C, Handel T, Wang L. 2004. Structural determinants of heparan sulfate interactions with Slit proteins. *Biochem Biophys Res Commun*. 317:352–357.